

# Long-Lived Non-Equilibrium Interstitial-Solid-Solutions in Binary Mixtures

Ioatzin Ríos de Anda

*H.H. Wills Physics Laboratory, Tyndall Ave., Bristol, BS8 1TL, UK and  
Centre for Nanoscience and Quantum Information, Tyndall Avenue, Bristol BS8 1FD, UK*

Francesco Turci

*H.H. Wills Physics Laboratory, Tyndall Ave., Bristol, BS8 1TL, UK*

Richard Sear

*Department of Physics, University of Surrey, Guildford, Surrey GU2 7XH, UK*

C. Patrick Royall

*H.H. Wills Physics Laboratory, Tyndall Ave., Bristol, BS8 1TL, UK  
School of Chemistry, Cantock's Close, University of Bristol, BS8 1TS, UK and  
Centre for Nanoscience and Quantum Information, Tyndall Avenue, Bristol BS8 1FD, UK  
(Dated: February 20, 2017)*

We perform particle resolved experimental studies on the heterogeneous crystallisation process of two component mixtures of hard spheres. The components have a size ratio of 0.39. We compared these with molecular dynamics simulations of homogenous nucleation. Surprisingly, we found for both experiments and simulations that the final assemblies are not the fixed composition binary and one-component crystals predicted by previous simulation work [Trizac *et al.*, *Mol. Phys.* **90**, 675 (1997)]; we instead observed interstitial solid solutions, where the large particles form crystalline close-packed lattices, whereas the small particles occupy random interstitial sites. This interstitial solution resembles that found when the small particles are only 0.3 of the larger particle's diameter [Filion *et al.*, *Phys. Rev. Lett.* **107**, 168302 (2011)]. However, unlike these smaller size ratios, simulations showed that the small particles are trapped in the octahedral holes of the ordered structure formed by the large particles, leading to long-lived non-equilibrium structures, not the equilibrium interstitial solutions found earlier. Interestingly, the percentage of small particles in the crystal formed by the large ones rapidly reaches a maximum of  $\sim 14\%$  for all the packing fractions tested and no further hopping of the former particles was observed. Non-equilibrium interstitial solid solutions are common, steel is one example, and so our results are relevant to a wide range of systems whose properties depend on a complex interplay of crystalline order and compositional disorder.

## I. INTRODUCTION

Among the most important properties of solids are their mechanical properties. Manipulating their mechanical properties is a central theme of materials science [1]. One key method for increasing the strength of a crystal lattice is to add one or more further species to form a *solid solution*. When the inclusions reside between the host lattice sites, an *interstitial* solid solution is formed. Steel is a hugely important example of such an interstitial solid solution (ISS) [2], in which the iron atoms form an ordered crystal lattice, with the smaller carbon atoms in the interstices. Substitutional solid solutions (SSS) are also important, there the second component is not in the interstices between atoms of the first component, but substitutes for atoms of the first component, on the lattice. Very recent developments in electron microscopy have for the first time allowed us to analyse the disorder of an SSS of iron in platinum [3]. Also, High Entropy Alloys (HEAs), which are effectively a multi-component SSS, are currently very actively studied as they are among the toughest materials known [4–8].

Hard spheres, as epitomised by colloids, are widely used as models to study the self-assembly and phase

behaviour processes of atoms and molecules. Since the structural evolution of colloidal suspensions can be followed in real space by means of confocal imaging, their study has allowed us to monitor the crystallisation process of different systems [10]. Additionally, the equilibrium structures of such processes have also been successfully characterised in simulations, which is crucial for fundamental understanding and for many applications, including material sciences, metallurgy, and biotechnology [11, 12]. The most popular example of these systems is monodisperse hard spheres, where the particles interact only by hard-core repulsions and whose phase behaviour has been widely studied, through both simulations and experiments [6]. These studies have identified the face-centered cubic (fcc) -often in a random mixture with hexagonal close packing (hcp)-, as the solid stable structure [5, 13].

Crystallisation of polydisperse colloidal mixtures has acquired more interest, as these present a richer and more complex phase behaviour than their monodisperse counterpart [5, 9, 13–16]. Amongst these systems, we find binary mixtures of hard spheres, which are composed of two populations of spheres of differing sizes. Similar to monodisperse hard spheres, they are also the simplest

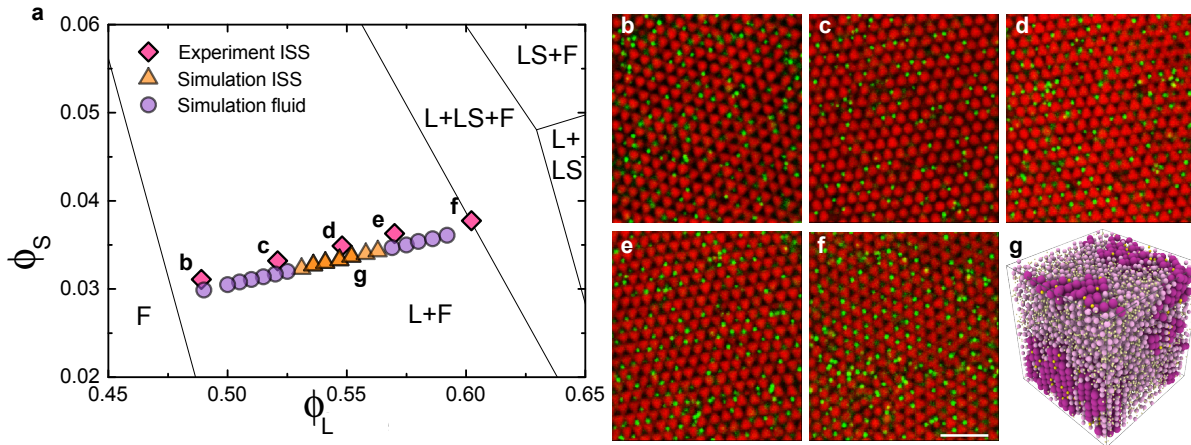


FIG. 1. (a) The state points we study (symbols), and Trizac, *et al.* [9]’s phase diagram of binary hard spheres with a size ratio  $\gamma = 0.414$ , in the  $\phi_L$ - $\phi_S$  plane. Diamonds: ISS from heterogeneous nucleation experiments. Purple circles: simulations that did not crystallise. Orange triangles: ISS from simulations. Snapshots: (b-f) crystalline structures found on experiments for the different  $\phi_{\text{tot}}$  tested, where the red and green colours correspond to large and small particles, respectively; (g) a representative ISS found for simulations with  $\phi_{\text{tot}} = 0.586$ , where crystalline large and small particles are coloured purple and yellow, respectively, whereas fluid large and small particles appear in light pink and light yellow, respectively. Scale bar = 10  $\mu\text{m}$ .

polydisperse colloidal system and thus, form a reference model to study phase transitions of mixtures [5, 9, 13, 15]. Crystals of these systems were observed by Sanders and Murray back in 1978, whilst analysing the microscopic structure of gem opals, which are composed of silica colloids and had an structure analogue to  $\text{AlB}_2$  and  $\text{NaZn}_{13}$  [17]. So far, both experimental and simulation studies have identified that the phase diversity found in binary mixtures depends on the size ratio of the components, the number ratio and total concentration of the particles [5, 6, 18, 19]. These studies have produced structures resembling the ones found in nature for different salts like  $\text{NaCl}$ ,  $\text{NaZn}_{13}$ ,  $\text{AlB}_2$  [5, 9, 15, 16, 18], the Laves structures  $\text{MgCu}_2$ ,  $\text{MgNi}_2$ ,  $\text{MgZn}_2$  [5, 6, 17], and most recently, stable ISS [5]. This large diversity of equilibrium structures highlights their potential for applications in photonics, optics, semiconductors and structure design [5, 9, 15, 18]. In addition, due to their simplicity, binary hard sphere mixtures are ideal models to study the kinetics of crystallisation in salts, metal alloys, metallic glasses and any other crystallising system where there is more than one species, and so there is a compositional variable [4–8].

However, only a few experimental studies have focused on the crystallisation *process* of binary hard spheres, which can be due to the difficulty of obtaining close-packed ordered structures. This is related to slow kinetics, caused by a competition of the crystal nuclei growth and compositional fluctuations. In addition, differences in sedimentation rates between the particles also play an important role in preventing crystallisation. [15, 20–22] Similar to one-component systems, the particles in the crystalline structure have a higher translational entropy than in the metastable fluid, which compensates for the

decrease of entropy as the system becomes more ordered [9, 13, 15, 16, 22]. In addition, it has been proposed that the theoretically predicted structures will only be thermodynamically stable if their maximum close packing fraction exceeds the correspondent 0.7405 for fcc or hcp lattices of one-component systems [9, 13, 15, 22].

Interestingly, these studies have also shown some discrepancies between the experimental observations and the predicted assemblies for particular size ratios and compositions, especially at concentrations near the glass transition [5, 13, 22]. Furthermore, the kinetic contributions to crystallisation, along with microscopic mechanisms that yield the ordering of mixtures are not yet fully understood [22], accentuating the complexity of these systems over one-component ones, and limiting their promising applications. Based on the interest in understanding such crystallisation processes, our goal is to study experimentally the heterogeneous crystallisation of a mixture of colloidal hard spheres at the particle-resolved level and compare our results with previous predictions. We also use simulations to study the evolution of the crystals, in particular the dynamics of the small particles, and propose a mechanism for the crystal formation.

This paper is organised as follows. In section II we describe the methodology used for both experiments and simulations, along with the structure analysis. In section III we first present the results for crystallisation for our experiments and their structural analysis. We compare such results with previous work. We continue with the structural analysis of the structures found on the simulations and the study of the evolution and quality of the crystals. We finalise by proposing a crystallisation mechanism for our system following the results obtained

through simulations. In the last section IV we present with our conclusions.

## II. METHODS

### A. Experiments

Sterically stabilised poly(methylmethacrylate) (PMMA) particles fluorescently labeled with different dyes and with a size ratio ( $\gamma = \sigma_S/\sigma_L$ ) of 0.39, were suspended separately in a solvent mixture that matches the density and refractive index of the particles. Additionally, tetrabutylammonium bromide (TBAB) salt was added in order to screen the charges, conditions that allow the particles to behave very close to hard spheres [18, 23, 24]. The suspensions were left to equilibrate for several hours, after which they were mixed together at a fixed number particle ratio,  $N_L/N_S=1$ , and at several total volume fractions,  $\phi_{\text{tot}}$ . These were calculated based on the amount of particles and solvent weighted. After shaking, the samples were confined to squared glass capillaries of 0.50 x 0.50 mm (Vitrocom) and sealed at each end with epoxy. The samples were studied by means of confocal laser scanning microscopy, CLSM (Leica SP5 fitted with a resonant scanner) using two different channels at 543 nm and 488 nm and NA 63x oil immersion objective. For particle tracking, 3D data sets were recorded by taking a full scan of the capillary in the  $z$  axis, making sure the pixel size was equal in all axes. We used particle tracking studies to determine the crystalline structure. The crystallisation time was calculated in Brownian time units for the large particles, i.e., the time it takes for the large spheres to diffuse a particle radius, given by  $\tau_B = (\sigma_L/2)^2/6D = 0.963s$ , where  $D$  is the diffusion constant. The Brownian time  $\tau_B$  thus sets our unit of time. Observations were carried out for over a month, which corresponds to  $2.6 \times 10^6 \tau_B$ , and were made all along the length and height of the capillaries, which were left standing in a vertical position.

### B. Simulations

Simulations were carried out using the open-source event-driven molecular dynamics DynamO package[25, 26] in isothermal-isochoric (NVT) conditions for a binary mixture. The total number of particles is  $N_{\text{tot}}=10\,968$  of equal mass,  $m=1$ . The size and number ratio, as well as the total particle densities were chosen to match the ones from the experiments, thus  $\gamma=0.39$  and  $\phi_{\text{tot}}$  from 0.52 to 0.64, respectively. A crystalline NaCl-type lattice (interpenetrating large and small FCC lattices) is used as the initial configuration, which is then melted and equilibrated or “relaxed” to the appropriate packing fractions until an equilibrated structure was found. Simulation times were scaled to sim-

ulation data following the relationship  $\tau_\alpha = 2.597 \tau_B$  used previously when comparing event-driven MD simulation and colloid experiments [27]. To confirm the validity of this approach for our binary system, we calculated the structural relaxation time  $\tau_\alpha$  of the large particles from the trajectories at  $\phi_{\text{tot}}=0.38$ . This we did by computing the intermediate scattering function (ISF),  $F(k, t) = N^{-1} \langle \sum_{j=1}^N \exp[-ik \cdot (x_j(t) - x_j(0)) \rangle$ . In order to characterise the mobility in the lengthscale of a particle diameter, we evaluated the wavenumber  $k$  at  $2\pi/\sigma$ [27, 28]. We obtained a value of  $\tau_\alpha=0.526$ , which is similar to the correspondent to one-component systems at the same packing fraction of  $\tau_\alpha=0.404$  obtained in the case of a one-component system [27].

### C. Identification of the local structure of the ISS

In order to determine the local ordering of the crystals formed in our experiments, we analysed separately the structures formed by each component through particle tracking. To locate the particles in the experiments, 3D data sets were directly analysed using the algorithm described in Leocmach and Tanaka[29]. Briefly, the coordinates of the particles are determined by convolving the original images to obtain blurred ones, where the bright spots of the former (corresponding to the particles’ centres) appear like bright blobs in the latter, which can be then filtered and detected. Further analysis of the crystalline structure for both experiments and simulations, was done by obtaining the bond orientational order parameters (BOO), based on complex spherical harmonics[30]. This analysis gives information of the degree and type of ordering, thus enabling us to differentiate between distinct crystalline phases. We focused on the locally averaged order parameters  $\bar{q}_4$  and  $\bar{q}_6$  for square and hexagonal orders, respectively, following the methodology described elsewhere[30, 31]. The nearest-neighbour cutoff used was determined as the contact distance between the first neighbours, obtained through the pair distribution function of the crystalline structure.

### D. Determination of the Quality of the Crystals

Following the long-range crystalline analysis described in [32, 33], we determined in both experiments and simulations, the typical crystalline domain size as  $N_Q = N^{-1} \langle \vec{Q}^* \cdot \vec{Q} \rangle$ , where  $N$  is the total number of particles and  $\vec{Q} = \sum_{p=1}^N \vec{q}_6(p)$ , the sum over all particles of the complex vector  $\vec{q}_6(p)$ , which is the projection of the bonds a particle  $p$  makes with its neighbours onto the spherical harmonics with  $l=6$ .  $\vec{q}_6(p)$  was previously normalised assuming  $p$  are oriented equally– thus belong to the same domain– by  $\vec{q}_6(p) \cdot \vec{q}_6(p)^* = 1$ . The values taken by  $N_Q$  will depend on the amount of particles oriented in the same fashion, with large clusters making a large contri-

bution, and thus giving large numbers for the former. In contrast, small values of  $N_Q$  will then indicate the presence of small crystallites.

### III. RESULTS AND DISCUSSION

#### A. Analysis of the crystalline structures: identification of Interstitial Solid Solutions (ISS)

In a pioneering study, Trizac and collaborators studied simulations of a mixture of binary hard spheres with a comparable size ratio [9] to the one presented herein. Their phase diagram, according to the partial packing fractions of each species, is reproduced in Fig. 1, where symbols represent our experimental state points for the experiments on heterogeneous nucleation (diamonds) and simulations (circles). According to their predictions, the equilibrium phases expected were 50:50 composition binary crystals (LS)— where the large and small particles form interpenetrating lattices— in coexistence with crystals of large spheres (L) and a fluid phase (F) for our most concentrated mixture. For the rest of the samples, only L and F are the expected equilibrium phases. We did not observe any of these structures. Instead, we found crystalline structures built up by the large particles with interstitial small particles positioned in a random fashion (Snapshots Fig. 1), regardless of the  $\phi_{\text{tot}}$  and in coexistence with a fluid phase for both the experiments and the simulations. Surprisingly, we did not find ordered structures for the simulations below  $\phi_{\text{tot}}=0.563$  or above  $\phi_{\text{tot}}=0.610$ , where the mixtures did not crystallised (Fig. 1 purple circles). The effect of polydispersity in highly concentrated samples of hard spheres was studied previously through event driven molecular dynamics simulations and showed that the former can increase the volume fraction at which crystallisation is observed by  $\sim 1\%$ [34]. For heterogeneous nucleation, the crystals grew parallel to the walls of the capillaries and the fluid phase was present far away from the walls. The presence of a flat wall clearly facilitates the nucleation process and thus the mixture is able to crystallise in a  $\phi_{\text{tot}}$  range larger than the simulations, where the nucleation starts in the bulk.

The ordered structures found are stable (ISS)[35], at least on the timescales we consider. In these, the crystals grow from the fluid phase and form ordered structures composed by the larger particles forming a close packed crystal, and the smaller particles in the interstices. The composition of these crystals is much poorer in the small particles than it is in the original fluid, where the number ratio is one. [5, 36].

Reasons for the discrepancy between our results and the ones obtained by Trizac *et al.* were hinted previously by Filion and collaborators in their simulations and experimental work on binary mixtures of hard spheres with size ratio  $\gamma = 0.3$ [5]. In this work, the authors identified ISS as the stable structure for different com-

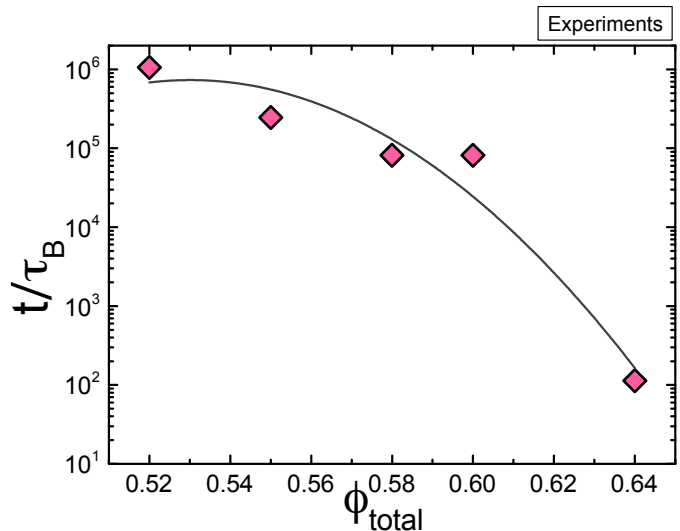


FIG. 2. Experimental results of the heterogeneous crystallisation time of the binary system in terms of Brownian motion,  $\tau_B$ . The line is a guide to the eye.

positions when the system was close-packed, whereas at low pressures binary crystals were observed. Additionally, they proposed that ISS could have been ignored by Trizac and collaborators, since a closer look to their results does show the presence of small particles within the crystal formed by the large ones. Our results support this suggestion and clarify this controversy by showing the presence of ISS where only crystals of large spheres were expected.

The heterogeneous crystallisation of our mixtures was studied as a function of the total volume fractions  $\phi_{\text{tot}} = \phi_L + \phi_S$  and we found that increasing this parameter increases the crystallisation rate, as shown in Fig. 2. This observation is in agreement with one component systems [11].

#### 1. Local structure of the large particles

According to the size ratio and for most of our samples, the equilibrium structure expected is a crystal formed by only the large particles (L) in coexistence with a fluid phase (F). For our most concentrated sample,  $\phi_{\text{tot}}=0.640$ , which lies close to the phase boundary, a NaCl-type crystal is also expected. In this type of crystal, the large components form a fcc lattice, with the small particles sitting on the octahedral sites and thus forming an interpenetrating sublattice with the same ordering. However, NiAs-type crystals can also be found, the difference being that in this case a hcp lattice is formed by the large particles [5, 15, 18]. The results of the analysis of the crystals formed only by the large particles for the experiments are summarised in Fig. 3, where we can observe that the crystalline phases consist of a mixture of fcc and hcp lattices, also known as random close

packed structure (rhcp) in coexistence with a fluid phase for all the total volume fractions tested. This random stacking has been identified before in experiments of heterogeneous nucleation of one-component systems [11].

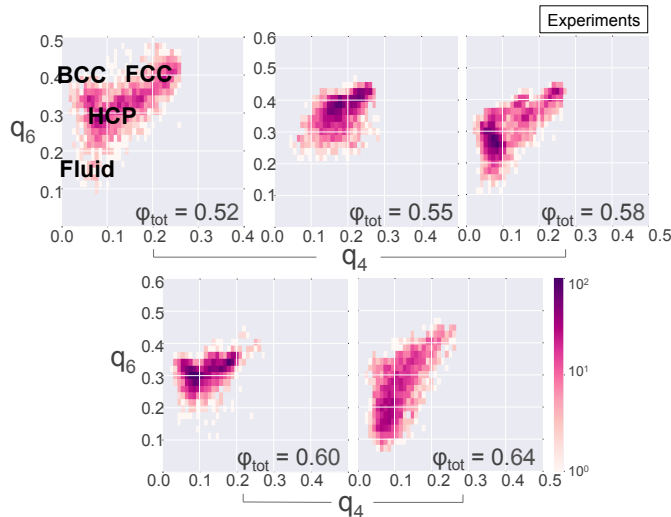


FIG. 3. Local bond order parameter diagrams for the crystalline phase found in experiments, showing fcc, hcp and fluid coexistence throughout the all the samples tested. The values for perfect bcc, fcc, hcp lattices are showed.

## 2. Local environment of the small particles: an analysis on the crystal quality and the vacancies in simulations

As discussed previously, the small particles are situated randomly in the octahedral holes of the fcc and hcp lattices formed by large particles, therefore no crystalline structure is detected when the small particles are analysed on their own. However, studying their local environment can give us information about the vacancies (defects) found in our ISS, and how they might depend on the total volume fraction. Furthermore, in the case that the size ratio is 0.3, Filion *et al.* showed that the small particles are able to hop at low pressures—where the system is not close-packed—, fill all the octahedral holes and yield a NaCl structure[5]. Conversely, in our experiments at size ratio is 0.39, we never observed any hopping of the small particles in direct imaging. Due to the limitations on tracking the motion of the small particles and to follow the evolution of the ISS in the experiments, we decided to conduct hard sphere molecular dynamics simulations in order to quantify the vacancies and follow accurately the time evolution of the crystalline structure.

Strikingly, and as mentioned above, the first phenomenon we observed was that the range of total packing fractions that crystallised *on the simulation timescale* was smaller than that of the experiments as seen in Fig. 1. Moreover, the total amount of crystalline structure ( $N_{Xtot}$ ) showed an initial increase with the growing  $\phi_{tot}$ , reaching the highest amount around 18% at  $\phi_{tot}=0.580$ ,

after which it started to decrease, as shown in Fig. 4. Such behaviour is already more complex than for one component systems. The need for a higher  $\phi_{tot}$  to observe crystallisation on the simulation timescale ( $\phi_{tot}=0.563$  in comparison with  $\phi=0.53$  for one component systems[37]) might be due to a higher free energy barrier to generate nuclei necessary for crystallisation. Furthermore, when experiments for homogenous nucleation were carried out, only one experiment underwent crystallisation, and that was at  $\phi_{tot}=0.55$ . This is consistent with observations by Hunt and coworkers for a related binary system with a similar size ratio, which also showed difficulties to crystallise[15]. Based on literature values for the equivalence between simulation and Brownian time—previously mentioned on the methods section[27]—, we estimated the crystallisation time for our experiments for homogenous nucleation and we found it to be two orders of magnitude larger than the corresponding crystallisation time in simulations. We limit our experimental timescale to a month ( $2.6 \times 10^6 \tau_B$ ), thus restricting our exploration of homogenous nucleation to simulations. Moreover the system size in the experiments is of order  $10^5$  times bigger than the simulations, suggesting a very substantial discrepancy in nucleation rates. Reasons for such a big discrepancy may arise as a consequence of inherent polydispersity of the PMMA particles, whose effect on increasing the nucleation time has been reported before for one component systems[38, 39]. Our findings suggest that this effect might be even bigger for binary mixtures. Additionally, Hunt *et al.* proposed that the lack of nucleation could be due to a large mismatch between the interfacial tension of the fluid and solid phase, which might be bigger in the binary system[15].

We also observed a drop of the crystalline fraction of our system at  $\phi_{tot}$  similar to the one where one-component systems exhibit slow dynamics  $\phi \simeq 0.58$ [8], related to the particles moving more slowly as their concentration increases, requiring a long time to rearrange in ordered structures. A similar trapping phenomenon could be happening here, where the particles do not move fast enough to rearrange and form crystals. Additionally,  $N_{Xtot}$  is low for all the packing fractions that crystallised, being less than 20% of the total particles in the system ( $N_{tot}$ ), which has been the cutoff percentage of a system in order to be called crystalline[38, 40].

Once we have identified ordered structures, we proceeded with analysing their structure, following the method used for the experimental data aforementioned. Likewise, we observed that the big particles formed a rhcp stacking in coexistence with a fluid, as can be observed in Fig. 5. Also, the small particles are present in an apparently random fashion within the octahedral holes. Such results indicate that regardless of the type of nucleation (homogenous or heterogeneous, for simulations and experiments, respectively) the structures found are comparable.

Klotsa and Jack defined a parameter  $N_Q$  to describe the size of coherent crystallites, i.e., what is the typical



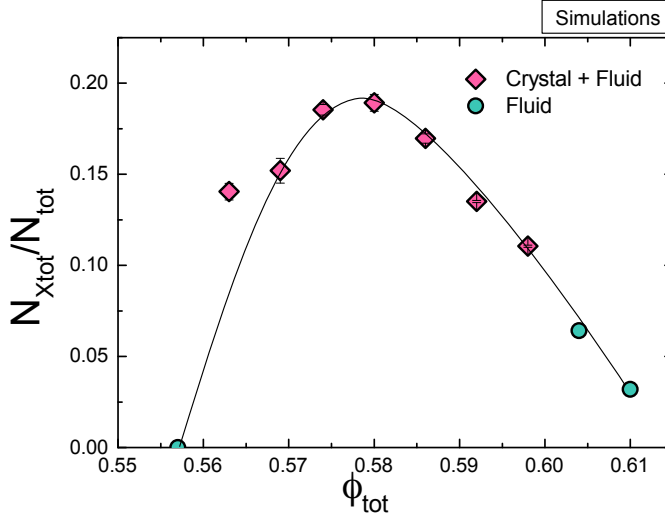


FIG. 4. Amount of total crystalline particles within the system according to their overall volume fraction,  $\phi_{\text{tot}}$  in simulations. The fitting line is a guide to the eye.

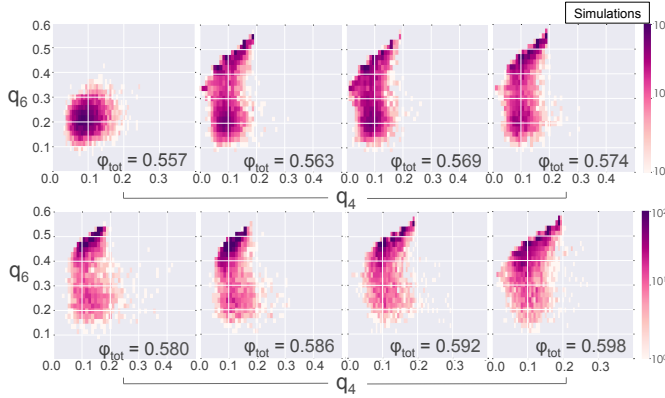


FIG. 5. Local BOO parameter diagrams for the crystalline phase found in simulations, showing rhcp and fluid coexistence throughout the samples with a crystalline order.  $\phi_{\text{tot}}=0.557$  is included to show the presence of only a liquid phase

number of particles in a coherently ordered crystal. We applied this analysis to both our experiments and simulations to determine which conditions yielded the crystals with the highest quality. In the case of the experiments, we analysed the crystals formed by the large particles, whereas for the simulations, we studied the evolution of  $N_Q$  through the crystallisation of the different samples. The results are presented in Fig. 6, where we compare this parameter with the number of large crystalline particles for the experiments, and with the total number of both large and crystalline particles for the simulations,  $N_X$ . It is evident from these results that the quality of the crystals obtained from heterogeneous nucleation in the experiments is higher than the homogenous nucleation present in the simulations, as  $N_Q$  presents significantly larger values in the former for similar  $N_X$ . Furthermore, the  $N_Q$  values for the experiments are close

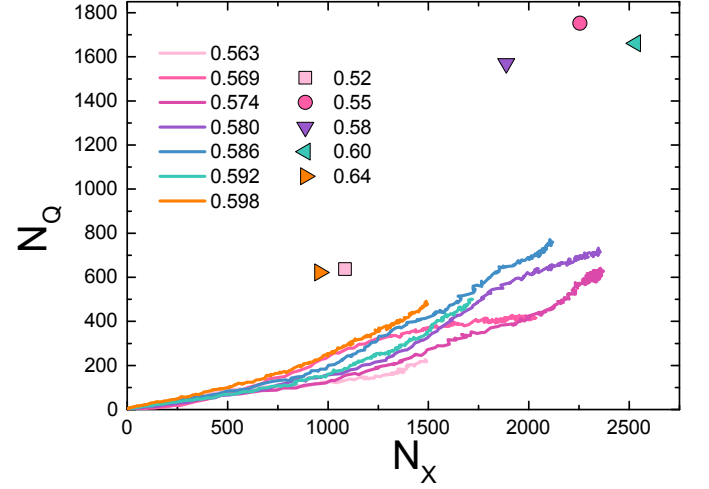


FIG. 6. Evolution of the measure of crystallinity  $N_Q$  throughout all the different packing fractions for simulations (lines) and experiments (symbols).  $N_Q$  shows that the quality of the crystals obtained in the experiments is higher than the simulations. For the experiments,  $N_X$  refers to the number of crystalline large particles, whereas for the simulations,  $N_X$  refers to both large and small crystalline particles.

to the number of crystalline particles. This could be a consequence of both the flat walls of the capillaries — as they serve as a template able to enhance the nucleation and layering of the particles and thus improve the orientation of the crystal[11] — or a consequence of longer waiting times. In the case of simulations, the numerical values of  $N_Q$  are significantly smaller than  $N_X$ , suggesting the presence of several clusters in all the samples. Also, a non-monotonic behaviour of this value is noted, since the highest values of the former do not correspond to the largest ones for the latter. This is evident for  $\phi_{\text{tot}}=0.598$ , whose maximum  $N_X$  surpasses the correspondent of  $\phi_{\text{tot}}=0.563$  that presents a similar  $N_X$ , and  $\phi_{\text{tot}}=0.569$  and  $0.592$ , with higher amounts of crystalline particles (Fig. 6 orange, pink, light pink and cyan lines, respectively). Interestingly, the dependence between these two parameters is not linear, with  $N_Q$  increasing faster than the crystal growth. A possible reason for this could be fast coalescence between the forming crystallites. Indeed,  $\phi_{\text{tot}}=0.574$  (Fig. 6 dark pink line) shows a flat region around  $N_X \sim 400$  followed by a further increase, which could be a consequence of two clusters merging to form a larger one.

We continued to analyse the nature of filling of octahedral interstices in our ISS. In order to do this, we calculated the aforementioned  $\bar{q}_6$  for the simulations on the whole system and focused only on the values obtained for the small component, since the local environment of a small particle in the octahedral hole is 6 large particles surrounding it. By plotting the distribution of populations with small and large values of  $\bar{q}_6$  (vacancy and occupancy, respectively), we can determine the value of  $\bar{q}_6$  corresponding to a particle in the octahedral site, and

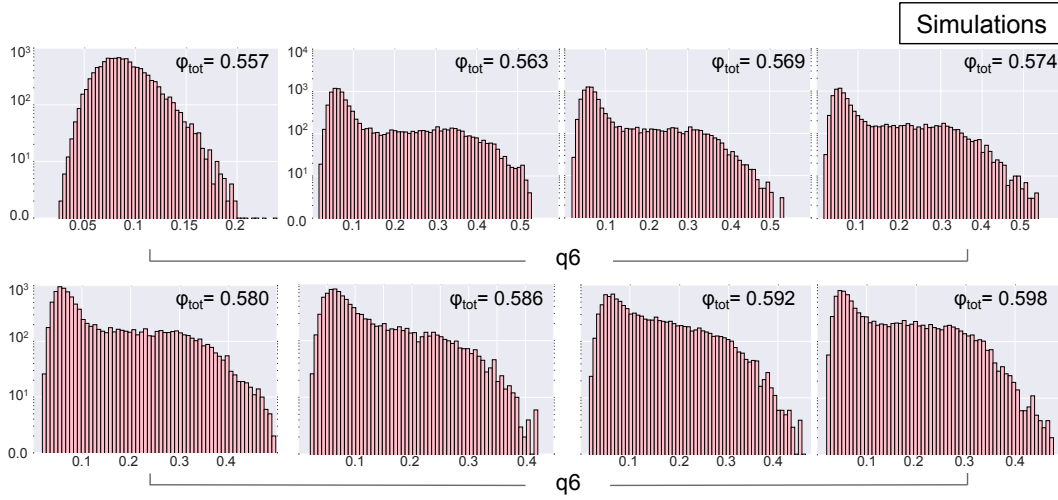


FIG. 7. Histograms of the  $\bar{q}_6$  values of the small particles surrounded by large ones for all the total volume fractions that crystallised in simulations, calculated following reference 30. The histograms show bimodal distributions with smaller second peaks on values of  $\bar{q}_6$  above 0.20 which correspond to small particles occupying the octahedral holes of the crystalline structure formed by the large particles. Note that  $\phi_{\text{tot}}=0.557$  does not crystallise.

use it to calculate the number of filled interstitial sites and thus the quality of our ISS. Such plots are presented in Fig. 7 where we can see that all of the samples that show crystalline structures present indeed a bimodal distribution, where values above 0.2 correspond to the interstitial particles, whereas samples that did not crystallise present a single-peaked distribution without any obvious shoulder and with values below 0.2.

We then followed the crystal growth by estimating the number of crystalline large ( $N_{\text{XL}}$ ) and small ( $N_{\text{XS}}$ ) particles, according to their  $\bar{q}_6$  values. These results are shown in Fig. 8 (a) and (b), respectively. Here, we observe that both quantities reach a plateau, indicating no further crystal growth and suggesting no hopping of the small particles within the interstitial sites of the fcc and hcp lattices, as discussed previously[5]. Next, we calculated the amount of  $N_{\text{XS}}$  relative to  $N_{\text{XL}}$  forming the ordered structure. We found two notable phenomena. Firstly, the octahedral holes are filled rapidly as the nucleation takes place (Fig. 8 (d)) with a maximum filling of the octahedral sites of around 14%, regardless of the packing fraction tested (Fig. 8 (c)). Secondly, we observed no further changes in the proportion of crystalline particles, suggesting a trapping effect. Since the number of small crystalline particles also reached a constant value, we infer that they become trapped (and immobilised) in the crystalline structure once it is formed.

### B. The dynamics of both large and small particles are arrested in the crystals

In order to show that our small particles were indeed immobilised, we computed the intermediate scattering function (ISF), as described previously[28] for the simulations with  $\phi_{\text{tot}}=0.586$  for geometrically selected large

and small particles in both liquid and crystalline regions. These results are shown in Fig. 9. We observe that both the large and small particles in the liquid region present movement, *i.e.* their ISF presents a behaviour typical for fluids (Fig. 9, dotted pink and purple lines, respectively). In contrast, both particles located in crystalline regions do not show any movement, identified as a non-decaying line on ISF (Fig. 9, continuous lines). We can conclude therefore that indeed, once the crystals are formed, the small particles are immobile within the crystal formed by the large particles; unable to hop and fill all the available octahedral holes, and thus our ISS remained as long-lived out-of-equilibrium structures.

### C. Proposed crystallisation mechanism

Previous experiments obtained for a related system with a size ratio, total volume fractions and stoichiometry, similar to those presented herein, have also identified the presence of a crystalline phase[15]. However, it was not possible to distinguish the type of crystalline lattice (fcc or hcp) these crystals presented, nor could the authors tell whether the vacancies of the lattice were fully occupied, or if their structures were also out-of-equilibrium ISS, since only one of the components of the system was analysed. Such limitations have been overcome here by applying particle resolved studies.

The crystalline phases analysed exhibit an apparently random close packing of the large particles, in agreement with previous predictions on one-component systems. In addition, long-ranged ordering analysis showed that these phases present low crystallinity, suggesting they are small crystalline clusters. We found that the small particles occupy the octahedral sites of the crystalline lattices in a

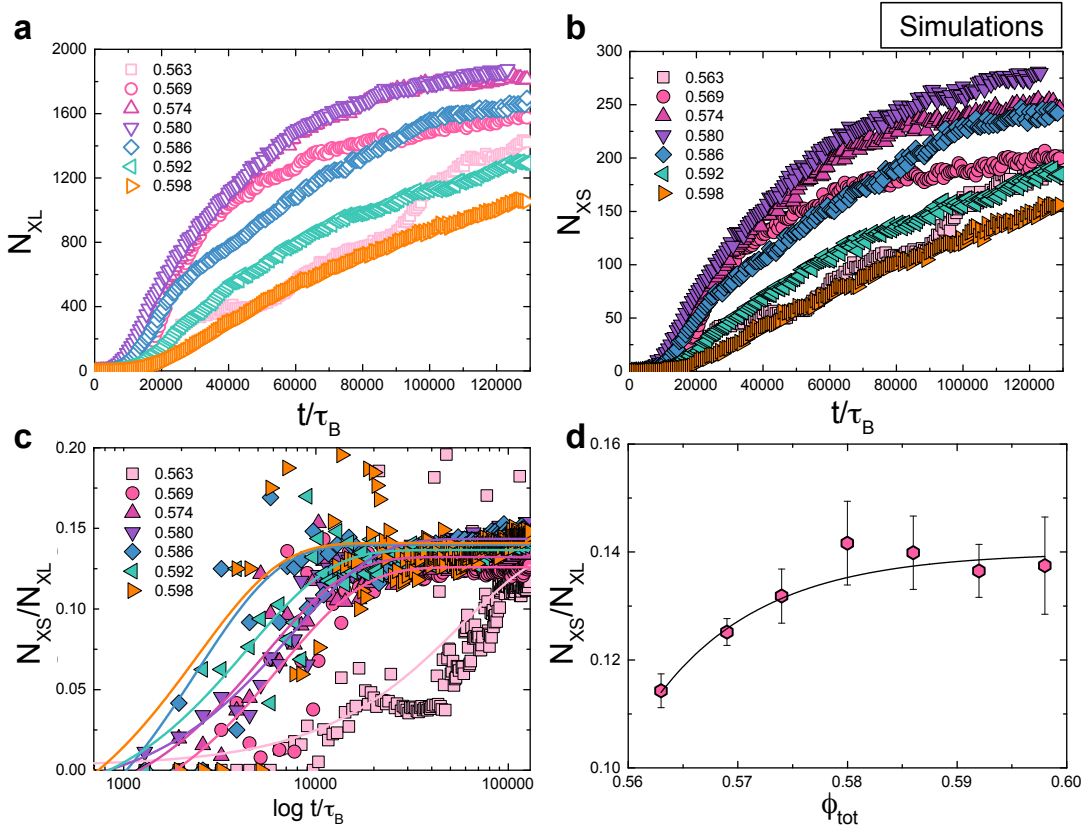


FIG. 8. The numbers of large (a) and small (b) crystalline particles as a function of time in simulations. (c) evolution of the proportion of small crystalline particles relative to the large crystalline ones in simulations according to their  $\phi_{tot}$ . (d) Averages of the percentage of small interstitial particles relative to the large ordered ones according to  $\phi_{tot}$ . The lines are a guide to the eye. The simulation time has been rescaled according to  $\tau_\alpha = 2.597 \tau_B$  (see Methods for details). Error bars correspond to standard deviation.

random fashion, forming a dilute ISS which consistently has a composition close to seven large particles for every one small particle. This has also been identified before in binary mixtures with a smaller size ratio of 0.3 compared to 0.39 here [5]. Filion and coauthors found that in order for the small particles to hop from one octahedral hole to the other, they needed to go through the adjacent tetrahedral hole ( $\sim 0.225\sigma_L$  across). Since the size ratio of our system surpasses that of the tetrahedral hole, the small particles have no access to said region and therefore they cannot hop, becoming trapped once the crystal of the large particles is formed, as above demonstrated. As mentioned above, one of the factors that may prevent crystal growth in binary mixtures is compositional fluctuations in the fluid. Therefore, one of the possible mechanisms for the kinetic frustration observed in our system can be the large and fast compositional changes that arise as a consequence of the exclusion of the small particles from the forming crystal. As the large particles rearrange independently in an ordered structure, some of the small particles become trapped in the octahedral holes. Such segregation increases the concentration of the latter in the fluid and thus inhibits further growth of the crystal.

#### IV. CONCLUSIONS

Interstitial solid solutions (ISS) were identified in both particle resolved experiments and simulations of a binary mixture with a size ratio of 0.39. These results are surprising as ISS were not predicted for a related system previously studied [9]. Through particle resolved studies carried out on the experimental results, we were able to identify that the crystalline structure was made up by the large particles forming a coexistent mixture of fcc and hcp lattices, with low crystallinity, and where the small particles are localised randomly within the octahedral holes. Simulations showed the same crystalline structure, and allowed us to follow the crystallisation process and quantify the amount of filling by the small particles. With this information, we were able to propose a crystallisation mechanism where firstly the large particles rearrange to form ordered structures independent of the small particles, which in turn become rapidly trapped within the growing crystal to a maximum of  $\sim 14\%$ . This large exclusion of the small particles generates large compositional fluctuations in the coexistent fluid and prevents further crystalline growth. Finally, we were able to show that the small particles are not able to pene-



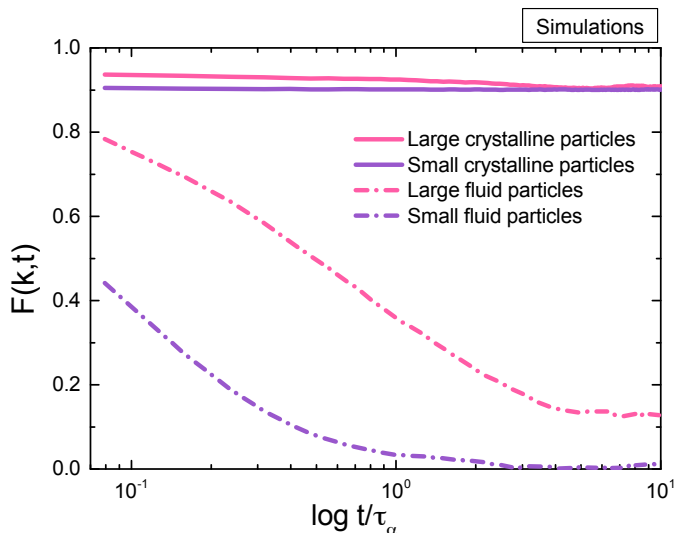


FIG. 9. ISFs from simulations, at  $\phi_{\text{tot}}=0.586$ . The large and small particles are shown in pink and purple, with continuous lines for particles identified as crystal, and dotted lines for particles identified as fluid. The simulations start at the end of a crystallisation simulation. Particles at the liquid-crystal boundary region were discarded in order to characterise only the crystalline and fluid particles.

trate the formed crystalline structure nor to move within the available octahedral holes, thus producing long-lived out-of-equilibrium ISS.

## V. ACKNOWLEDGEMENTS

IRdA would like to thank Conacyt for financial support. CPR acknowledges the Royal Society for funding and Kyoto University SPIRITS fund. FT and CPR acknowledge the European Research Council (ERC consolidator grant NANOPRS, project number 617266). This work was carried out using the computational facilities of the Advanced Computing Research Centre, University of Bristol.

## VI. REFERENCES

- [1] R. W Cahn. *The Coming of Materials Science*, volume 5 of *Pergamon Materials Series*. Pergamon, Oxford, 2009.
- [2] Verhoeven John D. *Steel metallurgy for the non-metallurgist*. Materials Park, Ohio : ASM International, 2007.
- [3] Yang Yongsoo, Chen Chien-Chun, Scott M. C., Ophus Colin, Xu Rui, Pryor Alan, Wu Li, Sun Fan, Theis Wolfgang, Zhou Jihan, Eisenbach Markus, Kent Paul R. C., Sabirianov Renat F., Zeng Hao, Ercius Peter, and Miao Jianwei. Deciphering chemical order/disorder and material properties at the single-atom level. *Nature*, 542(7639):75–79, 2017.
- [4] Bernd Gludovatz, Anton Hohenwarter, Dhiraj Catoor, Edwin H. Chang, Easo P. George, and Robert O. Ritchie. A fracture-resistant high-entropy alloy for cryogenic applications. *Science*, 345(6201):1153–1158, 2014.
- [5] L. Fillion, M. Hermes, R. Ni, E. C. M. Vermolen, A. Kuijk, C. G. Christova, J. C. P. Stiefelwagen, T. Vissers, A. van Blaaderen, and M. Dijkstra. Self-assembly of a colloidal interstitial solid with tunable sublattice doping. *Physical Review Letters*, 107(16):168302–, 10 2011.
- [6] L. Fillion. *Self-assembly in colloidal hard-sphere systems*. PhD thesis, Utrecht University, 2011.
- [7] Kai Zhang, W. Wendell Smith, Minglei Wang, Yanhui Liu, Jan Schroers, Mark D. Shattuck, and Corey S. O’Hern. Connection between the packing efficiency of binary hard spheres and the glass-forming ability of bulk metallic glasses. *Physical Review E*, 90(3):032311–, 09 2014.
- [8] C. Patrick Royall and Stephen R. Williams. The role of local structure in dynamical arrest. *Physics Reports*, 560:1–75, 2 2015.
- [9] E. Trizac, M. D. Eldridge, and P. MaMadden. Stability of the ab crystal for asymmetric binary hard sphere mixtures. *Mol. Phys.*, 90:675, 1997.
- [10] Alexei Ivlev, Hartmut Löwen, Gregor Morfill, and C. Patrick Royall. *Complex Plasmas and Colloidal Dispersions: Particle-resolved Studies of Classical Liquids and Solids*. World Scientific Co., Singapore Scientific, 2012.
- [11] Kirill Sandomirski, Elshad Allahyarov, Hartmut Lowen, and Stefan U. Egelhaaf. Heterogeneous crystallization of hard-sphere colloids near a wall. *Soft Matter*, 7(18):8050–8055, 2011.
- [12] Aaron E. Saunders and Brian A. Korgel. Observation of an ab phase in bidisperse nanocrystal superlattices. *ChemPhysChem*, 6(1):61–65, 2005.
- [13] A. B. Schofield, P. N. Pusey, and P. Radcliffe. Stability of the binary colloidal crystals  $\{a\}_2$  and  $\{a\}_{13}$ . *Physical Review E*, 72(3):031407–, 09 2005.
- [14] An T. Pham, Ryohei Seto, Johannes Schonke, Daniel Y. Joh, Ashutosh Chilkoti, Eliot Fried, and Benjamin B. Yellen. Crystallization kinetics of binary colloidal monolayers. *arXiv:1605.05389*, 2016.
- [15] N. Hunt, R. Jardine, and P. Bartlett. Superlattice formation in mixtures of hard-sphere colloids. *Physical Review E*, 62(1), 2000.
- [16] P. Bartlett, R. H. Ottewill, and P. N. Pusey. Superlattice formation in binary mixtures of hard-sphere colloids. *Phys. Rev. Lett.*, 68:3801, 1992.
- [17] J. V. Sanders and M. J. Murray. Ordered arrangements of spheres of two different sizes in opal. *Nature*, 275(5677):201–203, 09 1978.

- [18] E. C. M. Vermolen, A. Kuijk, L. C. Filion, M. Hermes, J. H. J. Thijssen, M. Dijkstra, and A. van Blaaderen. Fabrication of large binary colloidal crystals with a nacl structure. *Proceedings of the National Academy of Sciences*, 106(38):16063–16067, 2009.
- [19] Christina Christova. *Binary colloidal crystals*. PhD thesis, Utrecht University, 2005.
- [20] Esther Vermolen. *Manipulation of Colloidal Crystallization*. PhD thesis, Utrecht University, 2008.
- [21] K. P. Velikov, C. G. Christova, R. P. A. Dullens, and A. van Blaaderen. Layer-by-layer growth of binary colloidal crystals. *Science*, 26(5565), 2002.
- [22] M. D. Eldridge, P. A. Madden, P. N. Pusey, and P. Bartlett. Binary hard-sphere mixtures: a comparison between computer simulation and experiment. *Molecular Physics*, 84(2):395–420, 02 1995.
- [23] C. Patrick Royall, Wilson C. K. Poon, and Eric R. Weeks. In search of colloidal hard spheres. *Soft Matter*, 9(1):17–27, 2013.
- [24] C. P. Royall, A. A. Louis, and H. Tanaka. Measuring colloidal interactions with confocal microscopy. *J. Chem. Phys.*, 127:044507, 2007.
- [25] M. N. Bannerman, R. Sargant, and L. Lue. Dynamo: A free o(n) general event-driven simulator. *J. Comp. Chem.*, 32:3329–3338, 2011.
- [26] Marcus N. Bannerman and Leo Lue. Transport properties of highly asymmetric hard-sphere mixtures. *The Journal of Chemical Physics*, 130(16), 2009.
- [27] C. P. Royall, S. R. Williams, and H. Tanaka. The nature of the glass and gel transitions in sticky spheres. *ArXiv e-prints*, September 2014.
- [28] Andrew J. Dunleavy, Karoline Wiesner, Ryoichi Yamamoto, and C. Patrick Royall. Mutual information reveals multiple structural relaxation mechanisms in a model glass former. *Nature Communications*, 6:6089 EP –, 01 2015.
- [29] Mathieu Leocmach and Hajime Tanaka. A novel particle tracking method with individual particle size measurement and its application to ordering in glassy hard sphere colloids. *Soft Matter*, 9(5):1447–1457, 2013.
- [30] W. Lechner and C. Dellago. Accurate determination of crystal structures based on averaged local bond order parameters. *J. Chem. Phys.*, 129:114707, 2009.
- [31] I. Rios de Anda, A. Statt, F. Turci, and C. P. Royall. Low-density crystals in charged colloids: comparison with yukawa theory. *Contributions to Plasma Physics*, 55(2-3):172–179, 2015.
- [32] C. J. Fullerton and R. L. Jack. Optimising self-assembly through time-dependent interactions. *ArXiv e-prints*, September 2016.
- [33] Daphne Klotsa and Robert L. Jack. Controlling crystal self-assembly using a real-time feedback scheme. *The Journal of Chemical Physics*, 138(9):094502, 2013.
- [34] Emanuela Zaccarelli, Siobhan M. Liddle, and Wilson C. K. Poon. On polydispersity and the hard sphere glass transition. *Soft Matter*, 11(2):324–330, 2015.
- [35] Nicholas DeCristofaro and Roy Kaplow. Interstitial atom configurations in stable and metastable fe-n and fe-c solid solutions. *Metallurgical Transactions A*, 8(1
- [36] F. C. Campbell, editor. *Elements of Metallurgy and Engineering Alloys*, chapter Solid Solutions. Materials Park, OH: ASM International, 2008.
- [37] T. Schilling, H. J. Schoepe, M. Oettel, G. Opletal, and I. Snook. Precursor-mediated crystallization process in suspensions of hard spheres. *Phys. Rev. Lett.*, 105:025701, 2010.
- [38] J. Taffs, S. R. Williams, H. Tanaka, and C. P. Royall. Structure and kinetics in the freezing of nearly hard spheres. *Soft Matter*, 9:297–305, 2013.
- [39] Stefan Auer and Daan Frenkel. Suppression of crystal nucleation in polydisperse colloids due to increase of the surface free energy. *Nature*, 413(6857):711–713, 10 2001.
- [40] Jade Taffs and C. Patrick Royall. The role of fivefold symmetry in suppressing crystallization. *Nature Communications*, 7:13225 EP –, 10 2016.